

# Modelling the Skip-and-resurgence of Japanese Encephalitis Epidemics in Hong Kong

Shi Zhao, Yijun Lou, Alice P.Y. Chiu & Daihai He\*

Department of Applied Mathematics, Hong Kong Polytechnic University, Hong Kong

\* Correspondence to D.H.: [daihai.he@polyu.edu.hk](mailto:daihai.he@polyu.edu.hk)

May 14, 2018

## Abstract

Japanese encephalitis virus (JEV) is a zoonotic mosquito-borne virus, persisting in pigs, Ardeid birds and *Culex* mosquitoes. It is endemic to China and Southeastern Asia. The case-fatality ratio (CFR) or the rate of permanent psychiatric sequelae is 30% among symptomatic patients. There were no reported local JEV human cases between 2006 to 2010 in Hong Kong, but it was followed by a resurgence of cases from 2011 to 2017. The mechanism behind this “skip-and-resurgence” patterns is unclear.

This work aims to reveal the mechanism behind the “skip-and-resurgence” patterns using mathematical modelling and likelihood-based inference techniques. We found that pig-to-pig transmission increases the size of JEV epidemics but is unlikely to maintain the same level of transmission among pigs. The disappearance of JEV human cases in 2006-2010 could be explained by a sudden reduction of the population of farm pigs as a result of the implementation of the voluntary “pig-rearing licence surrendering” policy. The resurgence could be explained by of a new strain in 2011, which increased the transmissibility of the virus or the spill-over ratio from reservoir to host or both.

Keywords: Japanese encephalitis virus, mathematical modelling, skip-and-resurgence, vector-free transmission

## 1 Introduction

Japanese encephalitis virus (JEV) is a zoonotic and mosquito-borne virus that is the major cause of viral encephalitis in Asia. The annual total confirmed human cases has decreased substantially from 12,594 cases to 3,429 cases between 2006 and 2012, and then resurged to 5,399 in 2016 (Fig. 1). The case-fatality ratio and the rate of permanent neurologic or psychiatric sequelae of patients with encephalitis can be 30% [1, 3, 4, 5, 6, 7, 8] and over 35% in children [9]. JEV persists in a transmission cycle of pigs, Ardeid birds and mosquitoes. It could infect humans

25 through mosquito bites by *Culex tritaeniorhynchus* species [1, 4, 10]. Humans are dead-end hosts  
 26 where they cannot develop viremia to infect mosquitoes. Population sizes of farm pigs and the  
 27 size of rice land, which favors the *Culex* mosquitoes' growth, are the two key factors affecting local  
 28 transmission [1, 4, 11]

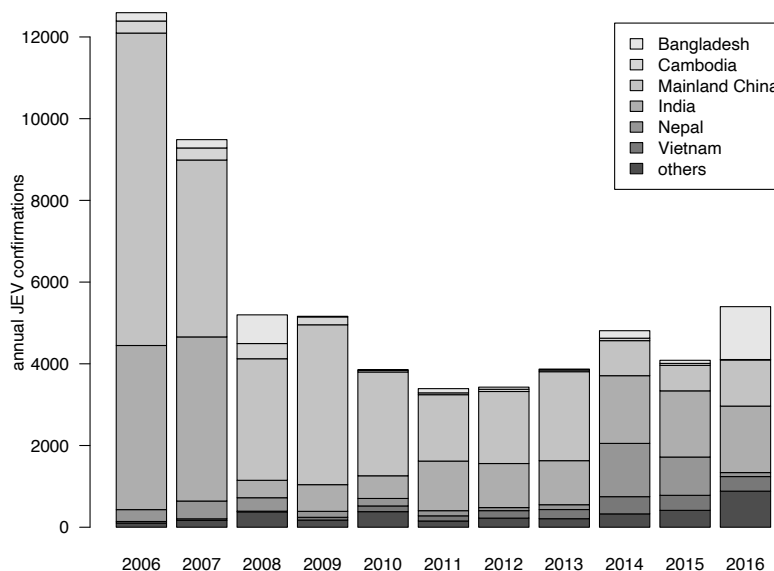


Figure 1: Annual JEV confirmations from 2006 to 2016 among the top six JEV endemic countries and the total of other countries. Data are obtained from World Health Organization [2].

29 Vertical transmission of JEV in mosquitoes and pig-to-pig transmission are the major de-  
 30 terminants of the following year's transmission. Vertical transmission exists between mosquitoes  
 31 and their eggs [12, 13, 14]. Mosquito population increases during spring, peaks in summer and  
 32 decreases during fall annually [16, 17]. According to a recent study by Ricklin et al., pig-to-pig  
 33 transmission is also present [15].

34 JEV transmission via blood transfusion has recently been found in Hong Kong, which was  
 35 probably the first case worldwide. The transmission was reported to come from an asymptomatic  
 36 viremic donor to two hospitalized patients [23].

37 Sero-prevalence of JEV antibodies varied by season among swines and among human pop-  
 38 ulation groups in Hong Kong. During rainy season between May and July, the sero-prevalence  
 39 among swines reached 91% compared with 34% that is reported in dry season [18]. It was ap-  
 40 proximately 80% to 90% among swines in July and August from 2000 to 2004 [16]. Another local  
 41 serological survey found that 23.5% of pig farmers and 5.9% of abattoir workers are seropositive  
 42 to JEV antibodies, in contrast to 0% reported among 30 blood donors [18].

43 JEV vaccine protection rates has been investigated. The vaccine was reported to have a  
 44 high effective protection rate of 93.3% by five years and a predicted protection rate of 85.5% by  
 45 10 years [20]. A recent study by Cao et al. investigated the current JEV vaccine derived from  
 46 G3 JEV genotype against the emerging G5 genotype in mice, and found that the lethal challenge  
 47 protection rate was 50%. The same study also reported that neutralizing antibodies against G5

48 JEV were detected in 35% of vaccinated healthy children [22].

49 Riley et al. examined the skip-and-resurgence patterns of JEV from 1969 to 2004 in Hong  
50 Kong [16]. They suggested that the skip from 1990 to 2002, except for one case reported in  
51 1996, was likely due to the lack of rice production, as *Culex* species breed principally in rice fields  
52 [29]. They proposed that the resurgence from 2003 to 2004 was likely due to the heightening of  
53 infectious disease notification system after the Severe Acute Respiratory Syndrome (i.e., SARS)  
54 outbreak in 2003 in Hong Kong [16].

55 In Hong Kong, no locally-acquired JEV case was reported between 2006 and 2010, but  
56 17 cases were reported between 2011 and June, 2017. Considering the declining local live pig  
57 population from 350,000 to 60,000 between 2004 and 2017 [24, 26, 25, 27, 28], the disappearance  
58 of local JEV cases between 2006 and 2010 are expected, but the resurgence of local cases is  
59 intriguing.

60 Our work aims to identify the mechanism underlying the JEV skip-and-resurgence patterns  
61 between December 2003 and May 2017 in Hong Kong. We hypothesized such behavior could be  
62 due to the surrendering of pig licenses during a pig rearing policy change in 2006 and/or a new  
63 JEV strain invasion around 2011. These hypotheses are tested using mathematical modelling and  
64 likelihood-based inference techniques.

## 65 2 Data and Methods

### 66 2.1 Data

67 The monthly JEV cases between December 2003 and May 2017 were retrieved online from the  
68 Centre for Health Protection in Hong Kong [30, 18]. The regional monthly mosquito ovitrap index  
69 from December 2003 to December 2016 were retrieved online from the Food and Environmental  
70 Hygiene Department in Hong Kong [31]. The annual pattern of reported JEV cases and regional  
71 mosquito ovitrap index are shown in Fig. 2. We present the time series of JEV cases and regional  
72 mosquito ovitrap index in Fig. 3.

73 The population sizes of live pigs in Hong Kong (Fig. 4) were obtained from local government  
74 reports, local news articles, and reports from Department of Agriculture in the United States  
75 [24, 35, 25, 28, 34, 32, 33, 26, 27]. Since the pig rearing license surrendering policy was implemented  
76 in May 2006, the number of local live pigs has rapidly declined. 243 out of 265 pig farms owners  
77 had surrendered their licenses [25].

### 78 2.2 JEV Compartmental Model

79 Ricklin et al. recently reported that pig-to-pig transmission of JEV can also occur without  
80 the mosquito vectors [15]. After the infectious period in pigs where JEV in swine serum are  
81 infectious to mosquitoes, there is also a convalescent period in which pig sheds JEV virus in  
82 their oronasal secretions. Thus, the pig population could be classified into five compartments:  
83 susceptible, exposed, infectious, convalescent and recovered which are denoted as  $S_p$ ,  $E_p$ ,  $I_p$ ,  $C_p$   
84 and  $R_p$  respectively. We considered pig-to-pig transmission and vector-borne transmission. Fig. 5  
85 shows the model diagram considering pigs, mosquitoes and humans. JEV transmission can be  
86 described by the following system of equations (Eqn. (1)).

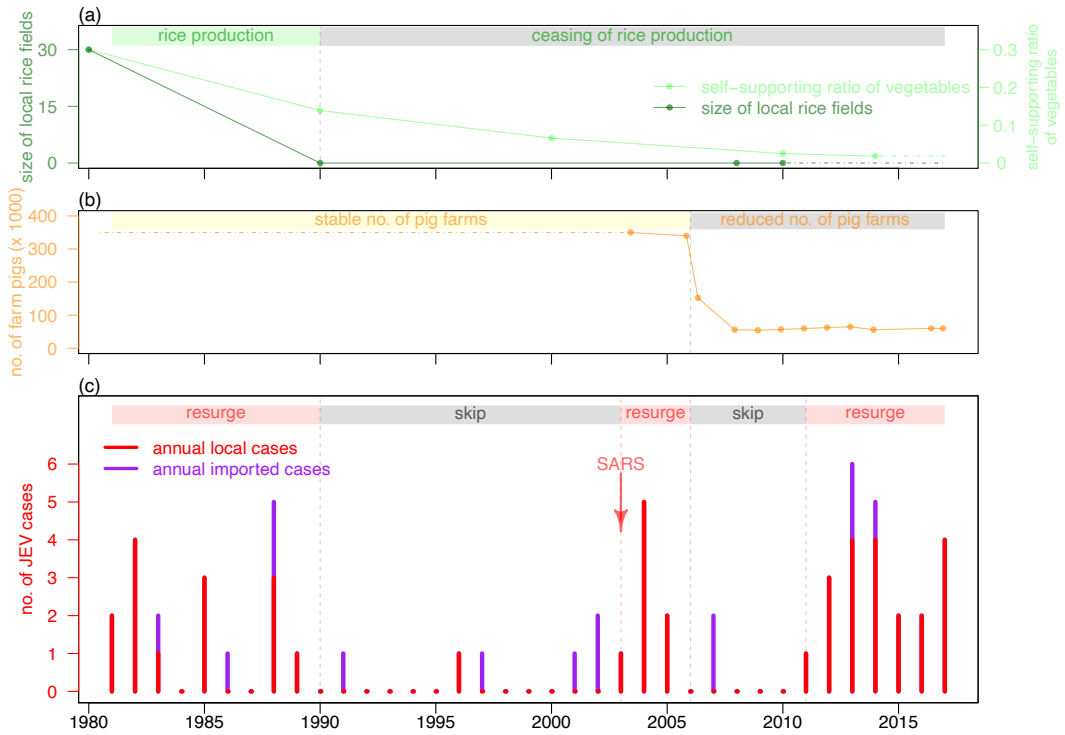


Figure 2: The plot of “skip-and-resurgence” of JEV epidemic from 1980 to 2017 in Hong Kong. Panel (a) shows the area of local rice production and self-supporting vegetable ratio. Panel (b) The orange line shows the number of local live pigs, where the data is obtained from Fig. 4. Panel (c) shows the reported annual (i.e. both local and imported) JEV cases in Hong Kong. The two blue arrows in panel (c) indicate the timing of H5N1 and SARS outbreaks respectively.

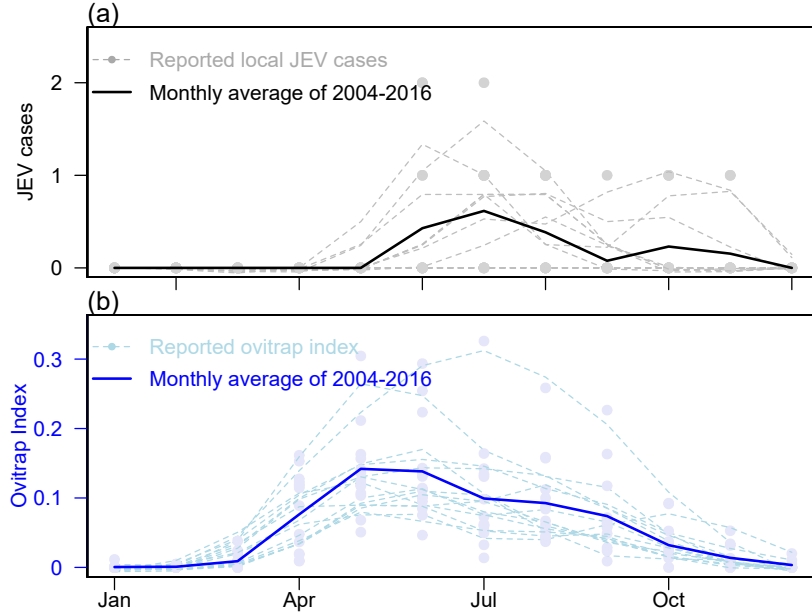


Figure 3: Panel (a) shows the monthly reported local JEV cases in Hong Kong, and panel (b) shows the average monthly oitrap index of regions (i.e., including Yuen Kong, Yuen Long and Tin Shui Wai) around Yuen Long district in Hong Kong. For both panels, darker lines represent annual averages, lighter lines represent smoothed data. Dots represent the annual reported data from 2004-2016.

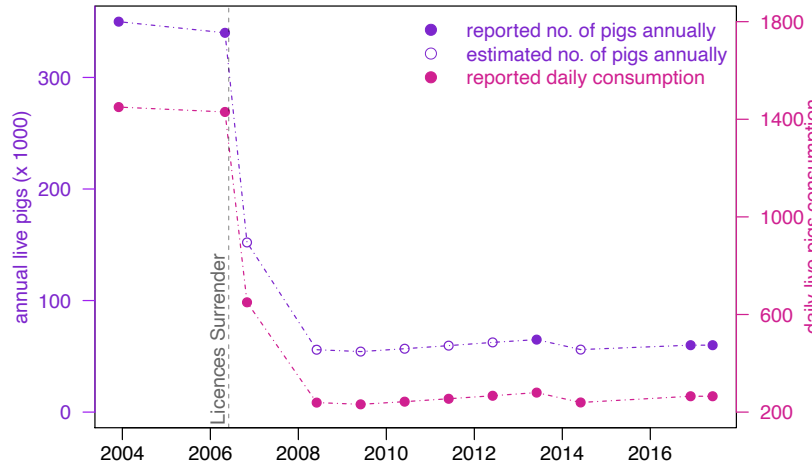


Figure 4: Local live pig populations and their daily consumptions from January 2004 to May 2017 in Hong Kong. Purple line represents the annual live pig populations, connected by their reported and estimated numbers, which are depicted in filled and hollow circles respectively ( $N_p$ ). Violet red line and dots represent the daily local live pig consumptions ( $\nu_p N_p$ ). Vertical grey dashed line denotes the time when the pig rearing license surrendering policy was implemented in Hong Kong.

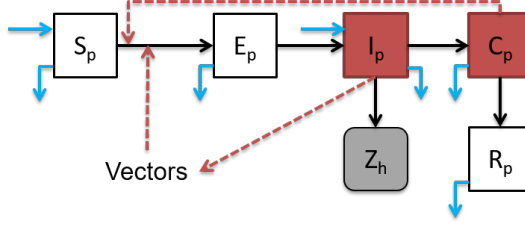


Figure 5: JEV model diagram. Infectious classes are denoted in red, and JEV human cases are in grey (i.e.,  $Z_h$ , or  $Z_i$  in Eqn. (2)). The transition paths are represented in black arrows. Red dashed arrows represent paths of transmission. Births and deaths (including slaughtering) of pigs are represented in light blue arrows.

$$\begin{cases} S'_p = (1 - \eta) \cdot B_p(t) \cdot N_p - \nu_p S_p - \left( \lambda_{vp} + \beta_p \cdot \frac{C_p}{N_p} \right) S_p, \\ E'_p = \left( \lambda_{vp} + \beta_p \cdot \frac{C_p}{N_p} \right) S_p - (\sigma_p + \nu_p) E_p, \\ I'_p = \eta \cdot B_p(t) \cdot N_p + \sigma_p E_p - (\gamma_p + \nu_p) I_p, \\ C'_p = \gamma_p I_p - (\delta_p + \nu_p) C_p, \\ R'_p = \delta_p C_p - \nu_p R_p. \end{cases} \quad (1)$$

87 Table 1 summarizes the model parameters in Eqns. (1). The effects of  $B_p(t)$  and  $\nu_p$  are presented  
 88 in the dynamics of local live pig population because  $N'_p = [B_p(t) - \nu_p]N_p$ . In this model, the total  
 89 pig population is:

$$90 \quad N_p = S_p + E_p + I_p + C_p + R_p,$$

91 where  $N_p$  is the observed live pig populations in Hong Kong and is a time-dependent parameter  
 92 (see purple dashed line in Fig. 4).  $B_p(t)$  is the time-dependent birth rate of local live pigs. Humans  
 93 are dead-end hosts and cannot further transmit the disease [1, 4, 11], thus we model human cases  
 94 using a variable spill-over ratio ( $\rho$ ) in week  $i$   $\rho_i$  (see Eqn. (2)):

$$Z_i = \int_{\text{week } i} \rho_i \gamma_p I_p dt. \quad (2)$$

95 Please see S2.2 for more reasoning on model structure.

96 We consider different scenarios (of new JEV strain invasion) to fit the “skip-and-resurgence”  
 97 pattern of the JEV epidemic. We refer to the invasion scenario with force of infection and spill-over  
 98 rate given respectively by equations (4) and (6) as in **I3** (see Table 3 and the main results). In  
 99 the Supplementary Information, we compare this invasion scenario with a baseline (no invasion,  
 100 see **B** in Table 3 and S1.1) and two alternative invasion scenarios (see **I1** and **I2** in Table 3, S1.3  
 101 and S1.2).

Table 1: Model input parameters. We denote JEV transmitted from vectors to pigs as “v→p”, and from pigs to humans as “p→h” respectively. Please see [S2.1](#) for more information of the initial proportions.

Parameters	Notations	Values	Ranges	Remarks/Units	Sources
Force of infection	$\lambda_{vp}$	-	time-dependent	v→p, per year	Eqn. <a href="#">(3)</a>
Latent period in pigs	$\sigma_p^{-1}$	1.5	1-2	days	<a href="#">[43]</a> <a href="#">[15]</a>
Infection period in pigs	$\gamma_p^{-1}$	3	2-4	days	<a href="#">[61]</a> <a href="#">[43]</a> <a href="#">[65]</a> <a href="#">[15]</a> <a href="#">[3]</a>
Convalescent period in pigs	$\delta_p^{-1}$	2.5	1-4	days	<a href="#">[15]</a>
Proportion of infected among imported pigs	$\eta$	1.0%	0.43%-1.45%	pigs, Nil	Eqn. <a href="#">(8)</a>
Effective contact rate	$\beta_p$	estimate	0.0-0.4	pigs, per days	Eqn. <a href="#">(10)</a>
Lifespan of pigs	$\nu_p^{-1}$	234.0	234.0	days	Eqn. <a href="#">(7)</a>
Population size of pigs	$N_p$	-	time-dependent	see Fig. <a href="#">4</a>	<a href="#">[24]</a> <a href="#">[26]</a> <a href="#">[25]</a> <a href="#">[27]</a> <a href="#">[28]</a> <a href="#">[18]</a>
Spill-over rate	$\rho$	-	time-dependent	p→h, Nil	Eqn. <a href="#">(5)</a>
Initial proportion of susceptible	$S_{p0}$	estimate	45-75%	Nil	<a href="#">[10]</a> <a href="#">[16]</a> <a href="#">[36]</a>
Initial proportion of exposed	$E_{p0}$	0.1%	-	Nil	assumed
Initial proportion of infectious	$I_{p0}$	0.1%	-	Nil	assumed
Initial proportion of convalescent	$C_{p0}$	0.1%	-	Nil	assumed
Initial proportion of recovered	$R_{p0}$	estimate	25-55%	Nil	<a href="#">[10]</a> <a href="#">[16]</a> <a href="#">[36]</a>

## 2.3 Model Framework

JEV cases were modelled as a Partially Observed Markov Process (POMP), also known as Hidden Markov model, using R package “POMP” [\[42\]](#). The iterated filtering and plug-and-play likelihood-based inference frameworks were employed to fit the time series [\[41\]](#), [\[40\]](#), [\[52\]](#). Furthermore, the Maximum Likelihood Estimate (MLE) was used to estimate the model parameters. To quantify the tradeoff between the goodness-of-fit of a model and its complexity [\[44\]](#), Bayesian Information Criterion (BIC) was used for model comparison. Simulations were performed by implementing the Euler-multinomial integration method with a fixed time-step of one day [\[48\]](#), [\[40\]](#).

The model was first validated with the observed JEV cases in Hong Kong, based on information about the size of pig population. Mosquito abundance is a time-dependent parameter, which was smoothed over time based on the ovitrap index ( $\omega$ ). The force of infection ( $\lambda_{vp}$ ) from vectors to reservoirs is another time-dependent parameter. The spill-over ratio ( $\rho$ ) is estimated through  $\omega$ .

The monthly observed cases,  $C_i$ , were assumed to follow a Poisson distribution (Poi), with a mean  $Z_i$ , the underlying monthly cases modelled by Eqn. [\(2\)](#). Hence, we have:

$$C_i \sim \text{Poi}(\lambda = Z_i) \quad \text{with} \quad \text{mean} : \mu_i = Z_i.$$

Thus, the overall log-likelihood function,  $l$ , was given by:

$$l(\Theta|C_1, \dots, C_n) = \sum_{i=1}^n \ln f(C_i|C_{1:(i-1)}, \Theta)$$

where  $\Theta$  denotes the parameter vector being estimated,  $f(C_i|C_{1:(i-1)}, \Theta)$  was the posterior probability measurement function for  $C_i$  given  $C_{1:(i-1)}$ , which were then numerically computed by Sequential Monte Carlo (SMC, also known as particle filtering) [\[40\]](#), and  $n$  denotes the total number of months during the study period.

122 Using the profile likelihood method, the confidence intervals (C.I.) of the model output  
 123 parameters were estimated based on the model input parameter ranges as described in Table 1.  
 124 Parameters estimation and statistical analyses are conducted using R (version 3.4.1) [19].

## 125 2.4 Parameter Estimation

126 **Force of Infection from Vectors to Reservoirs ( $\lambda_{vp}$ ):** We can express  $\lambda_{vp}$  as  $\lambda_{vp} =$   
 127  $a\vartheta_{vp} \cdot \frac{I_v}{N_p}$ , where  $a$  is the mosquito biting rate;  $\vartheta_{vp}$  is the transmission probability of JEV per  
 128 mosquito bite; and  $I_v$  is the number of infected mosquitoes. However, in this study, we simplify  
 129  $\lambda_{vp}$  as a function of ovitrap index over time, since we are employing a vector-free modelling  
 130 framework. This is justifiable by assuming that  $a$  and  $\vartheta_{vp}$  are constant, while  $\frac{I_v}{N_p}$  is roughly  
 131 proportional to the ovitrap index. Briefly, we assume:

$$\lambda_{vp} = k \cdot \omega(t) + b \quad (3)$$

132 where  $\omega$  is the time series of ovitrap index in Hong Kong,  $k$  and  $b$  are model parameters  
 133 under estimation. Constant  $b$  represents the contribution of the vertical transmission from adult  
 134 mosquitoes to their eggs. The vertical transmission ratio of *Culex tritaeniorhynchus* is varied from  
 135 12% to nearly 100% [13, 12]. By using Eqn. (3), we also incorporate the case that despite the  
 136 ovitrap index is close to zero during a dry season, the transmission rate can still be positive due  
 137 to vertical transmission of vectors.

138 To investigate the mechanism of the observed resurgence of JEV after 2011 in Hong Kong, we  
 139 partitioned the force of infection into time segments based on the hypothesis that the re-emergence  
 140 was due to the invasion of a new JEV strain. This hypothesis is then validated using statistical  
 141 approaches. We assume the force of infection ( $\lambda_{vp}$ ) takes the following form:

$$\lambda_{vp} = \begin{cases} k_1 \cdot \omega(t) + b, & t < T_0 \\ k_2 \cdot \omega(t) + b, & t \geq T_0 \end{cases} \quad (4)$$

142 where  $T_0$  is the time when the new JEV strain invaded.

143 Biologically, the force of infection ( $\lambda_{vp}$ ) under the new strain invasion scenario is higher than  
 144 the no-invasion scenario, since the pig population is immunologically naive in the first few years  
 145 after invasion. Thus, under the new-strain invasion hypothesis, we have  $k_2 > k_1 > 0$ . The average  
 146 spill-over ratio  $\langle \lambda_{vp} \rangle$  after invasion should be much higher than that before invasion. Without new  
 147 strain invasion, we have the special case where  $k_1 = k_2$  in Eqn. (4).

148 **Spill-over Ratio from Reservoirs to Humans ( $\rho$ ):** In Eqn. (2), we assume that humans  
 149 are dead-end hosts [1, 4, 11]. Thus, the reported JEV human cases are proportional to pig  
 150 infections according to the time-dependent spill-over ratio( $\rho$ ). Since the number of human cases  
 151 are related to the total number of vectors, we can further assume the spill-over ratio as a function  
 152 of ovitrap index:

$$\rho = \xi \cdot \omega(t - \tau) \quad (5)$$

153 where  $\xi$  is the strength of infectivity parameter under estimation and  $\tau$  is the sum of incubation  
 154 period of mosquitoes (i.e. 6 to 12 days) [36, 37, 13], latent period in humans (i.e. 5 to 13 days)  
 155 [4, 10, 3] and case-reporting delay. For simplicity, we fix  $\tau$  to be 15 days for this study.



156 To investigate the mechanism of the observed resurgence of JEV after 2011 in Hong Kong, we  
 157 partitioned the spill-over ratio into time segments based on the hypothesis that the re-emergence  
 158 was due to the invasion of a new JEV strain. This hypothesis is then validated using statistical  
 159 approaches. We assume the spill-over ratio ( $\rho$ ) takes the following form from Tien et al. [38]:

$$\rho = \begin{cases} \xi_1 \cdot \omega(t - \tau), & t < T_0 \\ \xi_2 \cdot \omega(t - \tau), & t \geq T_0 \end{cases} \quad (6)$$

160 where  $T_0$  is the time when the new JEV strain invaded.

161 Biologically, the spill-over ratio ( $\rho$ ) under the new strain invasion scenario is much higher  
 162 than the no-invasion scenario, since the pig population is immunologically naive in the first few  
 163 years after invasion. Thus, under the new-strain invasion hypothesis, we have  $\xi_2 > \xi_1 > 0$ .  
 164 The average spill-over ratio  $\langle \rho \rangle$  after invasion should be much higher than that before invasion.  
 165 Without new strain invasion, we have the special case where  $\xi_1 = \xi_2$  in Eqn. (6).

166 **Lifespan of pigs ( $\nu_p^{-1}$ ):** Hong Kong people consumed approximately 265 live domestic  
 167 pigs per day during 2016-17 [33, 32], and roughly 275 live domestic pigs per day in around 2012  
 168 [34], whereas the consumption was around 1,450 live domestic pigs back in 2004 [25]. The total  
 169 pig population has fallen from 350,000 in 2004-05 [24, 25, 26], to 65,000 in 2012 [27] and further  
 170 dropped to 60,000 in 2016-17 [28]. Thus the average lifespan of pigs  $\langle \nu_p^{-1} \rangle$  can be estimated as:

$$\begin{aligned} \text{During 2004-05 : } \langle \nu_p^{-1} \rangle &= \frac{N_p}{\text{daily consumptions}} = \frac{350000}{1450} \approx 241.38 \text{ days,} \\ \text{In 2012 : } \langle \nu_p^{-1} \rangle &= \frac{N_p}{\text{daily consumptions}} = \frac{65000}{275} \approx 236.36 \text{ days,} \\ \text{During 2016-17 : } \langle \nu_p^{-1} \rangle &= \frac{N_p}{\text{daily consumptions}} = \frac{60000}{265} \approx 226.42 \text{ days.} \end{aligned} \quad (7)$$

171 By averaging the above, we computed the average lifespan of pigs  $\nu_p^{-1}$  to be approximately 234  
 172 days.

173 **Pigs' population ( $N_p$ ):** Given that the average local living pig consumption is 650 live pigs  
 174 per day in 2007 [25], we approximate the total number of pigs ( $N_p$ ) to be  $234 \times 650 = 152,100$ .  
 175 The sudden drop in the number of live pigs between 2006 and 2007 was due to the surrendering of  
 176 pig rearing licenses in early 2006, which result in 243 out of 265 pig farm owners turning over their  
 177 licenses [25]. Although the daily live pig consumption is not included as a modelling parameter,  
 178 given the pig's average lifespan, we could infer the total number of live pigs from the amount of  
 179 daily consumption.

**Infection ratio among imported pigs ( $\eta$ ):**  $\eta$  can be computed as:

$$\eta = \langle \text{IAR}_p \rangle \cdot \frac{\gamma_p^{-1} + \delta_p^{-1}}{\langle \nu_p^{-1} \rangle}, \quad (8)$$

180 where  $\langle \text{IAR}_p \rangle$  is the average attack rate over the average lifespan of pigs  $\langle \nu_p^{-1} \rangle$ . According to  
 181 the value of parameter in Table 1, if  $\gamma_p^{-1}$  is 1.5 day,  $\delta_p^{-1}$  is 2.5 days,  $\langle \nu_p^{-1} \rangle$  is 234 days and  
 182  $\langle \text{IAR}_p \rangle \in [25\%, 85\%]$  [39, 10], we estimated that  $\eta \in [0.43\%, 1.45\%]$ .

183 **3 Results**

184 **3.1 Model Fitting Results**

185 In addition to the simulated median, we also present the simulated annual means of the  
 186 model prediction using the approach described in Camacho et al. [50], since simulated means  
 187 demonstrated fitting results more consistently when the data are being restricted as integers and  
 188 are subject to stochastic noise.

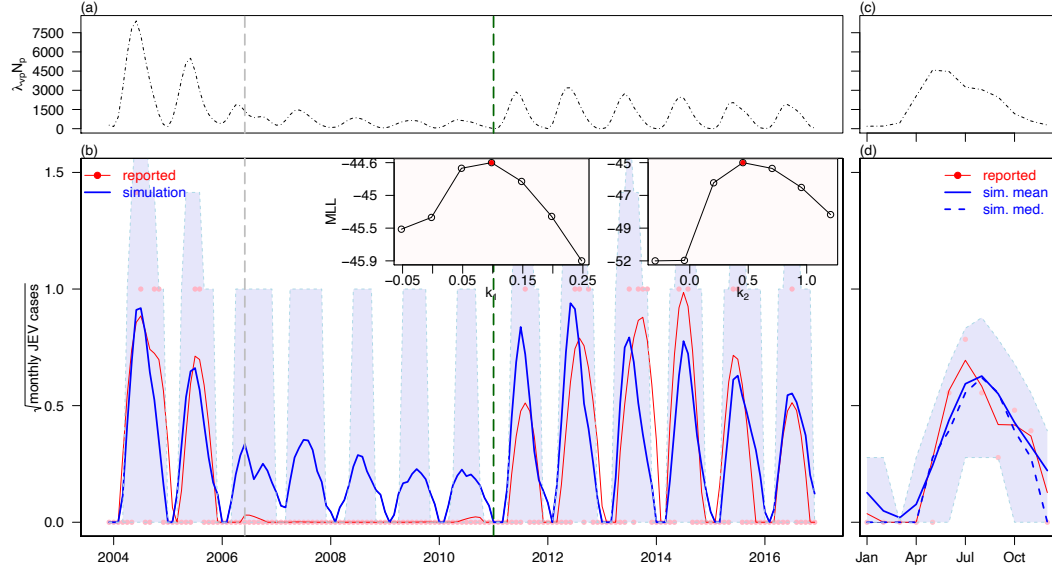


Figure 6: Model fitting results of JEV local cases in Hong Kong from 2004 to 2016 under new JEV strain invasion scenario with variable  $\rho$ . Panel (a) and (b) are the scaled force of infection (from vectors to pigs, scaled by the population size of pigs) and simulation results from 2004 to 2016 respectively. Panel (c) and (d) are the one-year-average scaled force of infection and simulation results from 2004 to 2016 respectively. In panel (a) and (b), black dashed lines are the scaled force of infection. In panel (b) and (d), blue lines are the simulation results, shaded regions are 95% quantile interval from simulation, pink dots are the reported (i.e., observed) JEV local cases and red lines are the smoothed (by *loess* function) reported JEV cases. The vertical grey dashed line marks the time point when Hong Kong government triggered the pig rearing licences surrender policy. The vertical dark green dashed line marks the time point when the new JEV strain introduced to the pigs’ population. The inset panel shows the maximum log-likelihood (MLL) values of different  $k_1$ s and  $k_2$ s, the red dot with the highest MLL are selected for fitting in main panels. The model scenario is associated with explanation **I3** in Table 3.

189 The model fitting results under the new JEV strain invasion scenario are shown in Fig. 6.  
 190 The estimated model parameters are summarized in Table 2. Although the long-term fitting  
 191 suffers from severe stochastic noise (i.e. zero, one or two cases per month), the 95% simulated  
 192 quantile interval covers all observed data, and the simulated average annual pattern is consistent  
 193 with the observed pattern.

194 BIC reduces more than 28 units when we went from the baseline (i.e. no invasion, see

Table 2: Summary table of model parameters' estimates under new JEV strain invasion scenario with both variable  $\lambda_{vp}$  and  $\rho$ .  $X_{p0}$  denotes the initial proportion of class  $X_p$ .

Parameter	Notation	Value	Type	Initial status	Unit/Remarks
Average force of infection	2004-10: $\langle\lambda_{vp}\rangle$	0.0043	estimated	time-dependent	before invasion
Average force of infection	2011-16: $\langle\lambda_{vp}\rangle$	0.0071	estimated	time-dependent	after invasion
Pig latent period	$\sigma_p^{-1}$	1.5	fixed	1-2	days
Pig infection period	$\gamma_p^{-1}$	3	fixed	2-4	days
Pig convalescent period	$\delta_p^{-1}$	2.5	fixed	1-4	days
Imported infection ratio	$\eta$	1.0%	fixed	0.43%-1.45%	Nil
Effective contact rate	$\beta_p$	0.0058	estimated	0.0-0.4	per days
Pig living period	$\nu_p^{-1}$	234	fixed	234	days
Pig population	$N_p$	-	-	time-dependent	pigs
Average spill over ratio	2004-10: $\langle\rho\rangle$	0.0002	estimated	time-dependent	before invasion
Average spill over ratio	2011-16: $\langle\rho\rangle$	0.0013	estimated	time-dependent	after invasion
Average ovttrap index	$\langle\omega\rangle$	0.0564	given	time-dependent	Nil
Initial susceptible	$S_{p0}$	0.6470	estimated	45-75%	Nil
Initial exposed	$E_{p0}$	0.001	assumed	0.0-0.25%	Nil
Initial infectious	$I_{p0}$	0.001	assumed	0.0-0.25%	Nil
Initial convalescent	$C_{p0}$	0.001	assumed	0.0-0.25%	Nil
Initial recovered	$R_{p0}$	0.3400	estimated	25-55%	Nil
BIC	BIC	144.8174	estimated	-	Nil

195 **S1.1**) scenario to the new strain invasion scenario (see Fig. **6** and explanation **I3** in Table **3**). We  
196 modelled another new strain invasion scenario where only the force of infection  $\lambda_{vp}$  is partitioned  
197 (see explanation **I2** in Table **3** and **S1.3**). The BIC increases approximately 1.0 unit which implies  
198 an almost equivalent fitting performance to the main results (see Fig. **6** and explanation **I3** in  
199 Table **3**). The partitioned force of infection with no partition on spill-over ratio is presented in  
200 **S1.3** (see explanation **I2** in Table **3**). Another invasion scenario with time-dependent  $\lambda_{vp}$  and  $\rho$   
201 are investigated in **S1.2** (see explanation **I1** in Table **3**), and BIC increases 4.55 unit. The detailed  
202 model performance and explanation of are in Table **3** and Supplementary Information.

Table 3: Summary of model fitting results and associated trait(s) under different scenarios.

Label	Scenario and its trait(s)	BIC	$\Delta\text{BIC}^\dagger$	Remarks
<b>B</b>	baseline (no invasion)	168.7009	28.4376	see <b>S1.1</b>
<b>I1</b>	invasion ( $\rho$ changed since 2011)	140.2633	0.0	see <b>S1.2</b>
<b>I2</b>	invasion ( $\lambda_{vp}$ changed since 2011)	141.2743	1.0110	see <b>S1.3</b>
<b>I3</b>	invasion ( $\rho$ and $\lambda_{vp}$ changed since 2011)	144.8174	4.5541	see Fig. <b>6</b> , Table <b>2</b>

$\dagger$ :  $\Delta\text{BIC} = \text{BIC} - \text{BIC}_{\min}$ , where  $\text{BIC}_{\min}$  is the minimum of BICs of all scenarios. Here,  $\text{BIC}_{\min} = 140.2633$  (see **S1.2**).

### 203 3.2 Basic Reproduction Number of Pig-to-Pig Transmission

204 Using the next generation matrix method [45, 49], the basic reproduction number,  $\mathcal{R}_{pp}$ , of  
 205 pig-to-pig transmission is computed as:

$$\mathcal{R}_{pp} = \frac{\beta_p \gamma_p \cdot (\eta \nu_p + \sigma_p)}{[(1 - \eta)(\gamma_p + \delta_p + \nu_p)\nu_p + \gamma_p \delta_p](\nu_p + \sigma_p)}. \quad (9)$$

206 We consider that imported infections are rare ( $\eta \approx 0^+$ ), and both incubation period and  
 207 infection period of JEV in pigs are negligible (i.e.,  $\sigma_p^{-1} \approx 0^+$  and  $\gamma_p^{-1} \approx 0^+$ ). Then, it could  
 208 be seen that  $\mathcal{R}_{pp} \approx \frac{\beta_p}{\delta_p + \nu_p}$ , which is consistent with the standard SIR compartmental model [48].  
 209 We estimated  $\mathcal{R}_{pp}$  to be 0.0013 (95% C.I.: [0.00,0.31]) under the invasion scenario (see Fig. 7).  
 210 Furthermore, the range of effective contact rate,

$$\beta_p \in [0.0, 0.4], \quad (10)$$

211 (see Table 1 and 2) is set corresponding to  $\mathcal{R}_{pp} \in [0.0, 1.0]$ .

212 The range of  $\mathcal{R}_{pp}$  could be inferred from the followings: JEV sero-positive rates among pigs  
 213 quickly decreases in winter [16]. Mosquito abundance is almost zero during the same time period.  
 214 Thus, this indicates the vector-free transmission of JEV among pigs cannot persist. Therefore,  
 215  $\mathcal{R}_{pp}$  is less 1.0 and positive (i.e., greater than 0).

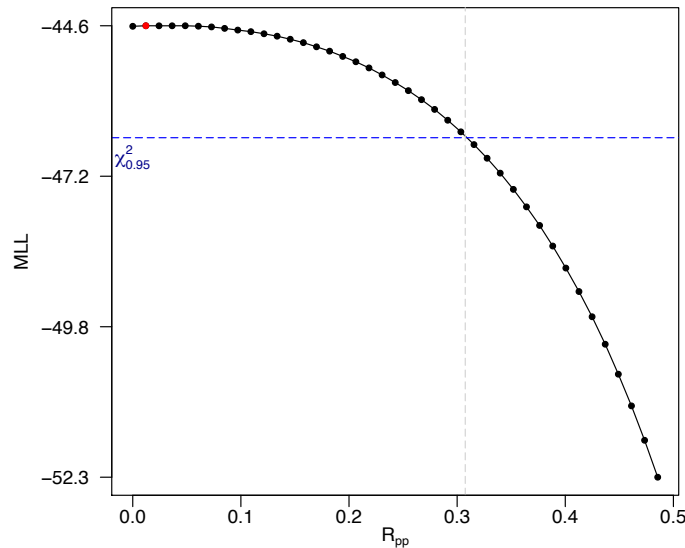


Figure 7: The results of estimation of the basic reproduction number of pig-to-pig transmission ( $\mathcal{R}_{pp}$ ) under new JEV strain invasion scenario with variable  $\rho$ . The horizontal blue dashed line is the 95% confidence threshold. The model scenario is associated with explanation **I3** in Table 3.

### 216 3.3 Critical Community Size

217 The critical community size (CCS) is defined as “the minimum size of a closed popula-  
 218 tion within which a host-to-host, non-zoonotic pathogen can persist indefinitely” [46]. Näsell [47]

219 presented a method of approximating the CCS from simple compartmental models of directly-  
 220 transmitted diseases. This is relevant to our study concerning pig-to-pig transmission. CCS can  
 221 be formulated (obtained from Eqn. 12.1 in Ref. [47]) as:

$$\text{CCS} \approx \frac{2\pi}{\ln 2} \cdot \frac{\mathcal{R}_0 \cdot \alpha_p^{1.5}}{(\mathcal{R}_0 - 1)^{1.5}}, \quad (11)$$

222 where  $\alpha_p = \frac{\gamma_p + \nu_p}{\nu_p}$  denotes the ratio of average lifespan of pigs ( $\nu_p^{-1}$ ) to the average duration of  
 223 infection. The basic reproduction number of pig-to-pig transmission,  $\mathcal{R}_{pp}$  in Eqn. (9) is relatively  
 224 small compared to that of vector-borne transmission,  $\mathcal{R}_{vp}$ . A modelling study by Khan et al.  
 225 estimated  $\mathcal{R}_{vp}$  to be 1.2 among pigs [39]. Also,  $\mathcal{R}_{vp}$  is believed to be greater than 1.0, as JEV  
 226 does spread during every rainy season. Applying the parameters under the new strain invasion  
 227 scenario in Table 2 (explanation **I3** in Table 3) to Eqn. (9),  $\mathcal{R}_{pp}$  is merely 0.0013, which is much  
 228 smaller than  $\mathcal{R}_{vp}$ . By using the next generation matrix approach [49, 52], the basic reproduction  
 229 number is:

$$\mathcal{R}_0 = \frac{\mathcal{R}_{pp} + \sqrt{\mathcal{R}_{pp}^2 + 4\mathcal{R}_{vp}^2}}{2}.$$

230 If we ignore the effects of  $\mathcal{R}_{pp}$  (i.e.,  $\mathcal{R}_{pp} \approx 0^+$  as in Ref. [52]), we have  $\mathcal{R}_0 \approx \mathcal{R}_{vp}$ . If we fix  
 231  $\nu_p^{-1} = 234.0$  (see Eqns. (7)), and set  $\mathcal{R}_0 \in [1.10, 1.40]$  and  $\gamma_p^{-1} \in [2.0, 4.0]$  (thus,  $\alpha_p \in [59.5, 118.0]$ ),  
 232 the relationship among  $\alpha_p$ ,  $\mathcal{R}_0$  and CCS (in Eqn. (11)) are illustrated in Fig. 8.

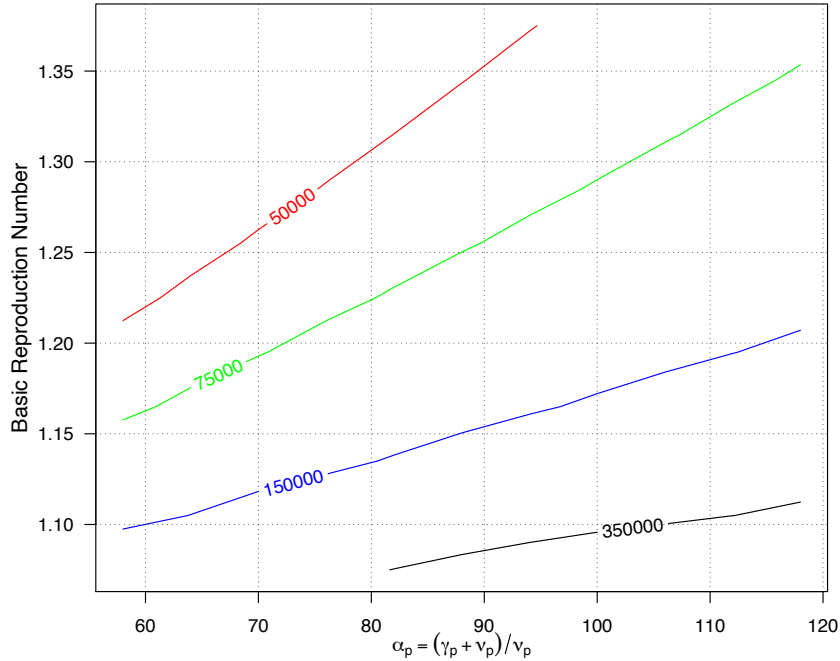


Figure 8: Contour plot of the relationships between critical community size (CCS),  $\alpha_p$  and the basic reproduction number  $\mathcal{R}_0$ . Numbers indicating the different CCS levels.

233 The number of local live pigs was reduced from 80,000 to 60,000 since 2008 after the pig  
 234 license surrendering policy came into effect (Fig. 4) [25]. With relatively low  $\mathcal{R}_0$ , CCS is greater

235 than 150,000 (see the area below the blue line in Fig. 8) over a broad range of  $\alpha_p$ 's. This could  
236 explain the local JEV case disappearance from 2006 to 2010 in Hong Kong.

237 Moreover, for the invasion scenario, we found that the force of infection,  $\lambda_{vp}$ , could increase  
238 after the introduction of new JEV strain while assuming a fixed spill-over ratio,  $\rho$ . The fitting  
239 results of the partitioned force of infection, which did not partition on the spill-over ratio, are  
240 presented in the S1.3 (see explanation I2 in Table 3). The goodness-of-fit is almost equivalent to  
241 the previous scenario. We modelled the partitioned  $\lambda_{vp}$  and  $\rho$  scenario in S1.2 (see explanation  
242 I1 in Table 3). Although the fitting results are not as good as in the invasion scenario, (i.e. the  
243 main results in Fig. 6 and explanation I3 in Table 3), it is still a significant improvement from  
244 the baseline (no invasion) scenario. The estimated force of infection,  $\lambda_{vp}$ , also increases after  
245 introducing a new JEV strain (see S1.2 and explanation I1 in Table 3). With an increased  $\mathcal{R}_0$   
246 due to an increased  $\lambda_{vp}$ , the CCS level could become lower than the local live pig's population  
247 level (see Fig. 8), which explains the resurgence of JEV cases. Further discussion on  $\mathcal{R}_0$  and CCS  
248 can be found in S2.3

## 249 4 Discussion

250 In this study, we argue that the resurgence of JEV after 2011 was likely due to new strain  
251 invasion that has a higher transmissibility. some indirect overseas evidence does exist: (i) **JEV**  
252 **genotype 1 (G1) strain since 2000:** In Southeast Asia, studies reported that Genotype 3  
253 was predominant during the late 20th century, and then genotype 1 started to replace genotype  
254 3 around 2000 and become dominant thereafter [60, 53, 7]. One genetic study found that the  
255 genotype 1 strain was not observed until 2008 in the regions of Mainland China surrounding Hong  
256 Kong [54]. Thus, it is very likely that there is a newly introduced JEV strain from pigs imported  
257 from these Mainland Chinese regions [63]; (ii) **JEV genotype 5 (G5) strain:** Similar JEV  
258 resurgences were observed in South Korea in 1998 and 2010 [62]. The resurgence in 1998 was  
259 likely due to the introduction of G1 strain in the mid-1990's [7, 54]. The first isolated local G5  
260 strain was reported in 2010 in South Korea, which coincided with the resurgence of JEV in 2010  
261 [64], where the average number of annual JEV cases increased approximately six- to eight-fold  
262 [62]. This is also consistent with our results of explanation I1 and I3 in Table 3.

263 We achieved almost equivalent goodness-of-fit under the two invasion scenarios. There are  
264 three potential explanations for the JEV resurgence since 2011: (I1) The newly introduced JEV  
265 strain has slightly increased the transmissibility from vectors to pigs, and considerably increased  
266 the spill-over ratio from pigs to humans; (I2) The newly introduced JEV strain has considerably  
267 increased the transmissibility, but the spill-over ratio is held constant; (I3) The main results:  
268 the newly introduced JEV strain has increased both the transmissibility and the spill-over ratio.  
269 Please also see the summary of I1-I3 in Table 3.

270 The symptomatic ratio of JEV could be further used to refine the mathematical model. As  
271 the majority of JEV infections are asymptomatic, and the mortality ratio for clinical JEV cases  
272 are approximately 30% (Table 4). We assume the symptomatic ratio of JEV among pigs are the  
273 same as that of humans, and asymptomatic pigs have negligible JEV transmissibility to vectors  
274 due to low within-host viral loads.

Our main results are derived from I3 (Fig. 6). In Table 2, we estimated the annual force of

Table 4: Symptomatic JEV infection ratio and case-fatality ratio (CFR) of JEV with clinical illness from various sources. The numbers in brackets are the geometric average of the upper and lower ranges.

$\frac{\text{Symptomatics}}{\text{Total Infections}}$ (Symptomatic%)	CFR = $\frac{\text{Mortality}}{\text{Clinical Illness}}$	Source(s)
(0.48%) 0.4%-0.5%	30%	[1, 3]
< 1%	20%-30%	[4, 5]
(0.81%) 0.33%-2%	25%	[6]
(0.63%) 0.1%-4%	25%-30%	[7, 8]
4% (occasionally)	-	[37]
(0.63%) 0.1%-4%	-	[58, 56, 51, 55, 57]
-	35%	[59]
-	36.4% (children)	[9]

infection  $\langle \lambda_{vp} \rangle$  to be 0.0042 and the proportion of susceptible pigs  $S_{p0}$  to be 68% at the beginning of each year [16, 36, 10], the annual average JEV infection attack rate ( $IAR_p$ ) among pigs could be computed as

$$IAR_p = \frac{\langle \lambda_{vp} \rangle \cdot S_{p0}}{\text{Symptomatic}\%}$$

275 where Symptomatic% is the JEV symptomatic rate, by which  $IAR_p$  is estimated from 35.26% to  
 276 59.50% (with Symptomatic%  $\in$  [0.48%, 0.81%]), which is consistent with [10, 16, 39]. The results  
 277 corresponding to **I2** are presented in [S1.3], where the annual transmission rate  $\langle \lambda_{vp} \rangle$  is set to be  
 278 0.0044 and 0.1763 before and after invasion, respectively. The larger annual force of infection  
 279 after invasion produces unreasonable  $IAR_p$ . With parameter values in [S1.3],  $\langle \lambda_{vp} \rangle = 0.1763$  and  
 280  $S_{p0} = 57.67\%$  lead to  $IAR_p \in [1255\%, 2118\%]$ , which is larger than 100%. The mechanism **I3**  
 281 implies increase in both  $\lambda_{vp}$  and  $\rho$  after invasion (see [S1.2]). With  $S_{p0} = 64\%$ ,  $IAR_p$  is increased  
 282 from [33.98%, 57.33%] to [56.10%, 94.67%] after invasion, within acceptable ranges. Therefore,  
 283 according to the range of  $IAR_p$ , **I1** and **I3** are likely to be the possible explanations of the  
 284 resurgence of JEV epidemics in 2011, while **I2** is unlikely since it predicts unreasonable values of  
 285  $IAR_p$ .

286 Furthermore, **I3** could be more biologically reasonable than **I1**. In **I1**, we assumed the force  
 287 of infection (i.e.,  $\lambda_{vp}$ ) unchanged but only change the value of spill-over rate before/after the new  
 288 JEV invasion. However, with the force of infection in **I1**, the JEV epidemic is unlike to maintain  
 289 according to the estimation results of CCS (i.e., in this case, the pig population is lower than the  
 290 CCS). On the contrary, with increased force of infection in **I3**, the JEV epidemic is very likely to  
 291 come back (i.e., resurgent) since 2011. Further work is needed in order to identify the biological  
 292 evidences and mechanisms of **I3**.

293 In this work, we only investigated the scenarios of new JEV invasion, more possible causes  
 294 (or scenarios) due to various other factors can be further explored.

## 5 Conclusions

We developed a simple mathematical model to investigate the mechanisms behind the skip-and-resurgence patterns of JEV human cases in Hong Kong. The critical community size (CCS) estimated through the model indicates that the pig rearing license surrender policy on May 2006 could be responsible for the disappearance of JEV human during 2006-10, assuming that other factors remain unchanged. Compared with the results of baseline (no invasion) scenario (see [SI.1](#)), our fitting results in the hypothetical scenario imply that the resurgence of JEV in 2011 was likely due to the introduction of new strains which has a higher transmissibility and/or a spill-over ratio.

The basic reproduction number ( $\mathcal{R}_{pp}$ ) of pig-to-pig transmission is estimated to be 0.0013 (95% C.I.: [0.00,0.30]). Although the vector-free JEV transmission route exists [\[15\]](#) and it could increase the epidemic size and prolongs the outbreak, JEV is unable to spread among pigs without vectors.

Thus vector control remains the most important and effective measure in mitigating JEV outbreaks in Hong Kong. Apparently, the reduction in local farm pig did not lead to elimination of JEV in Hong Kong. But monitoring JEV among pigs is still very important. This work shed light on the understanding of JEV epidemic in the other parts of Asia. A better understanding on the JEV epidemiology is helpful for strategies design and mitigation of JEV in other places. Our work shows that even though pigs play a very crucial role, a reduction of pigs might not be sufficient (to prevent JEV outbreaks).

## 6 Acknowledgement

The model simulations are performed on workstations of the Department of Applied Mathematics at the Hong Kong Polytechnic University. This work was partially supported by the Early Career Schemes ((PolyU 251001/14M) and (PolyU 253004/14P)) and General Research Fund (PolyU 153277/16P) from Hong Kong Research Grants Council. The authors would like to thank the editor and two anonymous reviewers for their comments and suggestions, which greatly improved the manuscript.

## References

- [1] World Health Organization. Japanese Encephalitis fact sheet. <http://www.who.int/mediacentre/factsheets/fs386/en/>. Accessed on Jul, 2017.
- [2] World Health Organization. Japanese Encephalitis annual incidence record. [http://apps.who.int/immunization\\_monitoring/globalsummary/timeseries/tsincidencejapenc.html](http://apps.who.int/immunization_monitoring/globalsummary/timeseries/tsincidencejapenc.html). Accessed on Apr, 2018.
- [3] Centers for Disease Control, R.O.C. (Taiwan), Japanese Encephalitis. <http://www.cdc.gov.tw/english/info.aspx?treeid=E79C7A9E1E9B1CDF&nowtreeid=E02C24F0DACDD729&tid=784CF7F674BD5DFA>. Accessed on Jul, 2017.



- 330 [4] Centers for Disease Control and Prevention (CDC). Japanese Encephalitis. <https://www.cdc.gov/japaneseencephalitis/index.html>. Accessed on Jul, 2017.  
331
- 332 [5] Arai S, Matsunaga Y, Takasaki T, Tanaka-Taya K, Taniguchi K, Okabe N, Kurane I, Vaccine  
333 Preventable Diseases Surveillance Program of Japan. Japanese encephalitis: surveillance and  
334 elimination effort in Japan from 1982 to 2004. *Jpn J Infect Dis.* 2008;61(5):333-8.
- 335 [6] Libraty DH, Nisalak A, Endy TP, Suntayakorn S, Vaughn DW, Innis BL. Clinical and  
336 immunological risk factors for severe disease in Japanese encephalitis. *Trans R Soc Trop  
337 Med Hyg.* 2002;96(2):173-8.
- 338 [7] Mackenzie JS, Gubler DJ, Petersen LR. Emerging flaviviruses: the spread and resurgence  
339 of Japanese encephalitis, West Nile and dengue viruses. *Nat Med.* 2004;10:S98-109.
- 340 [8] Solomon T, Winter PM. Neurovirulence and host factors in flavivirus encephalitis—evidence  
341 from clinical epidemiology. *Arch Virol Suppl.* 2004;(18):161-70.
- 342 [9] Kumar R, Mathur A, Kumar A, Sharma S, Chakraborty S, Chaturvedi UC. Clinical features  
343 & prognostic indicators of Japanese encephalitis in children in Lucknow (India). *Indian J  
344 Med Res.* 1990;91:321-7.
- 345 [10] Center for Health Protection. Japanese Encephalitis. <http://www.chp.gov.hk/en/content/9/24/28.html>. Accessed on Jul, 2017.  
346
- 347 [11] Impoinvil DE, Baylis M, Solomon T. Japanese encephalitis: on the one health agenda. In  
348 *One Health: The Human-Animal-Environment Interfaces in Emerging Infectious Diseases*  
349 *The Concept and Examples of a One Health Approach (Current Topics in Microbiology and*  
350 *Immunology, 365)*. Berlin, Heidelberg: Springer Berlin Heidelberg : Imprint: Springer.
- 351 [12] Rosen L, Lien JC, Shroyer DA, Baker RH, Lu LC. Experimental vertical transmission of  
352 Japanese encephalitis virus by *Culex tritaeniorhynchus* and other mosquitoes. *Am J Trop  
353 Med Hyg.*1989;40(5):548-56.
- 354 [13] Takashima I, Rosen L. Horizontal and vertical transmission of Japanese encephalitis virus  
355 by *Aedes japonicus* (Diptera: Culicidae). *J Med Entomol.* 1989;26(5):454-8.
- 356 [14] Rosen L, Tesh RB, Lien JC, Cross JH. Transovarial transmission of Japanese encephalitis  
357 virus by mosquitoes. *Science.* 1978;199(4331):909-11.
- 358 [15] Ricklin ME, Garcia-Nicolas O, Brechbuhl D, Python S, Zumkehr B, Nougairede A, Charrel  
359 RN, Posthaus H, Oevermann A, Summerfield A. Vector-free transmission and persistence of  
360 Japanese encephalitis virus in pigs. *Nat Commun.* 2016;7.
- 361 [16] Riley S, Leung GM, Ho LM, Cowling BJ. Identification of the key elements of transmission  
362 of Japanese encephalitis virus in Hong Kong. *RFID: 05050132.*
- 363 [17] Riley S, Leung GM, Ho LM, Cowling BJ. Transmission of Japanese encephalitis virus in  
364 Hong Kong. *Hong Kong Med J.* 2012;18 Suppl 2:45-6.

- 365 [18] Scientific Committee on Vector-borne Diseases, Hong Kong. official website. <http://www.chp.gov.hk/en/sas7/101/110/107.html>. accessed on Jul, 2017.
- 366
- 367 [19] R: The R Project for Statistical Computing. <https://www.r-project.org/>.
- 368 [20] Desai K, Coudeville L, Bailleux F. Modelling the long-term persistence of neutralizing anti-  
369 body in adults after one dose of live attenuated Japanese encephalitis chimeric virus vaccine.  
370 Vaccine. 2012;30(15):2510-5.
- 371 [21] Lam K, Tsang OT, Yung RW, Lau KK. Japanese encephalitis in Hong Kong. Hong Kong  
372 Med J. 2005;11(3):182-8.
- 373 [22] Cao L, Fu S, Gao X, Li M, Cui S, Li X, Cao Y, Lei W, Lu Z, He Y, Wang H. Low protec-  
374 tive efficacy of the current Japanese encephalitis vaccine against the emerging genotype 5  
375 Japanese encephalitis virus. PLoS Negl Trop Dis. 2016;10(5):e0004686.
- 376 [23] South China Morning Post website. [http://www.scmp.com/news/hong-kong/  
377 health-environment/article/2103667/hong-kong-tackles-worlds-first-case-patient](http://www.scmp.com/news/hong-kong/health-environment/article/2103667/hong-kong-tackles-worlds-first-case-patient).  
378 Accessed on Aug, 2017.
- 379 [24] Legislative Council of Hong Kong, Official Report (CB(2) 1663/05-06(05)). (URL) Accessed  
380 on Aug, 2017.
- 381 [25] Legislative Council of Hong Kong, Official Report (CB(2)2445/06-07(01)). (URL) Accessed  
382 on Aug, 2017.
- 383 [26] The Government of Hong Kong, Agriculture, Fisheries and Conservation Department  
384 (AFCD) official website. <http://www.afcd.gov.hk/eindex.html>. accessed on Jul, 2017.
- 385 [27] The Government of Hong Kong, Agriculture, Fisheries and Conservation Department  
386 (AFCD), Annual Reports. [http://www.afcd.gov.hk/misc/download/annualreport2012/  
387 agriculture.html](http://www.afcd.gov.hk/misc/download/annualreport2012/agriculture.html). accessed on Aug, 2017.
- 388 [28] Hong Kong 01, Press Release. (URL) Accessed on Aug, 2017.
- 389 [29] Tian HY, Bi P, Cazelles B, Zhou S, Huang SQ, Yang J, Pei Y, Wu XX, Fu SH, Tong SL, Wang  
390 HY. How environmental conditions impact mosquito ecology and Japanese encephalitis: an  
391 eco-epidemiological approach. Environ. Int. 2015;79:17-24.
- 392 [30] The Government of Hong Kong, Center for Health Protection (CHP), Statistics on com-  
393 municable diseases official website. <http://www.chp.gov.hk/en/notifiable1/10/26/43.html>.  
394 Accessed on Jul, 2017.
- 395 [31] The Government of Hong Kong, Food and Environmental Hygiene Department, Pest Control  
396 website. [http://www.fehd.gov.hk/english/safefood/dengue\\_fever/index.html](http://www.fehd.gov.hk/english/safefood/dengue_fever/index.html). Accessed  
397 on Jul, 2017.

- 398 [32] The Government of Hong Kong, Food and Environmental Hygiene Department (FEHD),  
399 Press Release official website. [http://sc.isd.gov.hk/gb/www.info.gov.hk/gia/general/  
400 201011/04/P201011040289.htm](http://sc.isd.gov.hk/gb/www.info.gov.hk/gia/general/201011/04/P201011040289.htm) and <http://www.fehd.gov.hk/english/index.html>. Accessed  
401 on Jul, 2017.
- 402 [33] The Government of Hong Kong, Food and Environmental Hygiene Department (FEHD),  
403 Monthly Average Daily Supply and Auction Prices of Live Pigs. [http://www.fehd.gov.hk/  
404 tc\\_chi/sh/data/supply\\_avg\\_tw.html](http://www.fehd.gov.hk/tc_chi/sh/data/supply_avg_tw.html). Accessed on Aug, 2017.
- 405 [34] Ta Kung Pao in Hong Kong, Press Release. (URL). Accessed on Aug, 2017.
- 406 [35] United States Department of Agriculture (USDA), Global Agriculture Information Network  
407 (GAIN) Reports. <http://www.usfoods-hongkong.net/res/mns/00321/HK1330.pdf> and [http://  
408 //www.usfoods-hongkong.net/res/mns/00433/HK1524.pdf](http://www.usfoods-hongkong.net/res/mns/00433/HK1524.pdf). accessed on Sep, 2017.
- 409 [36] Konno J. Cyclic outbreak of Japanese encephalitis among pigs and humans. Japanese Journal  
410 of Tropical Medicine. 1969;10(2):132-3.
- 411 [37] Van den Hurk AF, Ritchie SA, Mackenzie JS. Ecology and geographical expansion of  
412 Japanese encephalitis virus. Annu Rev Entomol. 2009;54:17-35.
- 413 [38] Tien JH, Poinar HN, Fisman DN, Earn DJ. Herald waves of cholera in nineteenth century  
414 London. J. R. Soc. Interface. 2010;rsif20100494.
- 415 [39] Khan SU, Salje H, Hannan A, Islam MA, Bhuyan AM, Islam MA, Rahman MZ, Nahar N,  
416 Hossain MJ, Luby SP, Gurley ES. Dynamics of Japanese encephalitis virus transmission  
417 among pigs in Northwest Bangladesh and the potential impact of pig vaccination. PLoS  
418 Negl Trop Dis. 2014;8(9):e3166.
- 419 [40] He D, Ionides EL, King AA. Plug-and-play inference for disease dynamics: measles in large  
420 and small populations as a case study. J R Soc Interface. 2010;7:271-83.
- 421 [41] King AA, Nguyen D, Ionides EL. Statistical inference for partially observed Markov processes  
422 via the R package pomp. J Stat Softw. 2016; 69:1-43.
- 423 [42] King AA. Statistical Inference for Partially-Observed Markov Processes. [http://kingaa.  
424 github.io/pomp/](http://kingaa.github.io/pomp/); accessed on Jun, 2017.
- 425 [43] Kodama K, Sasaki N, Inoue YK. Studies of live attenuated Japanese encephalitis vaccine in  
426 swine. J Immunol. 1968;100(1):194-200.
- 427 [44] Schwarz G. Estimating the dimension of a model. Ann Stat. 1978;6:461-4.
- 428 [45] Van den Driessche P, Watmough J. Reproduction numbers and sub-threshold endemic equi-  
429 libria for compartmental models of disease transmission. Math Biosci. 2002;180(1):29-48.
- 430 [46] Bartlett MS. The critical community size for measles in the United States. J. R. Stat. Soc.  
431 Series A (General). 1960:37-44.

- 432 [47] Nåsell I. A new look at the critical community size for childhood infections. *Theor Popul*  
433 *Biol.* 2005;67(3):203-16.
- 434 [48] Allen LJ, Brauer F, Van den Driessche P, Wu J. *Mathematical epidemiology. Lecture Notes*  
435 *in Mathematics.* 2008;1945:81-130.
- 436 [49] Brauer F, Castillo-Chavez C, Mubayi A, Towers S. Some models for epidemics of vector-  
437 transmitted diseases. *Infectious Disease Modelling.* 2016;1(1):79-87.
- 438 [50] Camacho A, Kucharski AJ, Funk S, Breman J, Piot P, Edmunds WJ. Potential for large  
439 outbreaks of Ebola virus disease. *Epidemics.* 2014;9:70-8.
- 440 [51] Chakraborty MS, Chakravarti SK, Mukherjee KK, Mitra AC. Inapparent infection by  
441 Japanese encephalitis (JE) virus in West Bengal. *Indian J Public Health.* 1980;24(3):121-7.
- 442 [52] Gao D, Lou Y, He D, Porco TC, Kuang Y, Chowell G, et al. Prevention and Control of  
443 Zika as a Mosquito-Borne and Sexually Transmitted Disease: A Mathematical Modeling  
444 Analysis. *Sci Rep.* 2016;6:28070.
- 445 [53] Gao X, Liu H, Li M, Fu S, Liang G. Insights into the evolutionary history of Japanese  
446 encephalitis virus (JEV) based on whole-genome sequences comprising the five genotypes.  
447 *Virol J.* 2015;12(1):43.
- 448 [54] Gao X, Liu H, Wang H, Fu S, Guo Z, Liang G. Southernmost Asia is the source of Japanese  
449 encephalitis virus (genotype 1) diversity from which the viruses disperse and evolve through-  
450 out Asia. *PLoS Negl Trop Dis.* 2013;7(9):e2459.
- 451 [55] Grossman RA, Edelman R, Chiewanich P, Voodhikul P, Siriwan C. Study of Japanese en-  
452 cephalitis virus in Chiangmai Valley, Thailand. II. Human clinical infections. *Am J Epi-*  
453 *demiol.* 1973;98:121-32.
- 454 [56] Grossman RA, Edelman R, Willhight M, Pantuwatana S, Udomsakdi S. Study of Japanese  
455 Encephalitis Virus in Chiangmai Valley, Thailand: III. Human seroepidemiology and inap-  
456 parent infections. *Am J Epidemiol.* 1973;98(2):133-49.
- 457 [57] Halstead SB, Grosz CR. Subclinical Japanese Encephalitis I. Infection of Americans with  
458 Limited Residence in Korea. *Am J Hyg.* 1962;75(2):190-201.
- 459 [58] Konishi E, Suzuki T. Ratios of subclinical to clinical Japanese encephalitis (JE) virus infec-  
460 tions in vaccinated populations: evaluation of an inactivated JE vaccine by comparing the  
461 ratios with those in unvaccinated populations. *Vaccine.* 2002;21(1):98-107.
- 462 [59] Monath TP, Levenbook I, Soike K, Zhang ZX, Ratterree M, Draper K, Barrett AD, Nichols  
463 R, Weltzin R, Arroyo J, Guirakhoo F. Chimeric yellow fever virus 17D-Japanese encephalitis  
464 virus vaccine: dose-response effectiveness and extended safety testing in rhesus monkeys. *J*  
465 *Virol.* 2000;74(4):1742-51.

- 466 [60] Pan XL, Liu H, Wang HY, Fu SH, Liu HZ, Zhang HL, Li MH, Gao XY, Wang JL, Sun XH,  
467 Lu XJ. Emergence of genotype I of Japanese encephalitis virus as the dominant genotype  
468 in Asia. *J Virol*. 2011;85(19):9847-53.
- 469 [61] Ricklin ME, Garcia-Nicolas O, Brechbuhl D, Python S, Zumkehr B, Posthaus H, Oevermann  
470 A, Summerfield A. Japanese encephalitis virus tropism in experimentally infected pigs. *Vet*  
471 *Res*. 2016;47(1):34.
- 472 [62] Sunwoo JS, Jung KH, Lee ST, Lee SK, Chu K. Reemergence of Japanese Encephalitis in  
473 South Korea, 2010!V2015. *Emerg Infect Dis*. 2016;22(10):1841.
- 474 [63] The Government of Hong Kong, Agriculture, Fisheries and Conservation Department  
475 (AFCD). Imported live pigs. [https://www.afcd.gov.hk/English/quarantine/qua\\_ie/qua\\_](https://www.afcd.gov.hk/English/quarantine/qua_ie/qua_ie_ipab/qua_ie_ipab_ilpbp/qua_ie_ipab_ilpbp.html)  
476 [ie\\_ipab/qua\\_ie\\_ipab\\_ilpbp/qua\\_ie\\_ipab\\_ilpbp.html](https://www.afcd.gov.hk/English/quarantine/qua_ie/qua_ie_ipab/qua_ie_ipab_ilpbp/qua_ie_ipab_ilpbp.html); Accessed on Aug, 2017.
- 477 [64] Takhampunya R, Kim HC, Tippayachai B, Kengluetcha A, Klein TA, Lee WJ, Grieco J,  
478 Evans BP. Emergence of Japanese encephalitis virus genotype V in the Republic of Korea.  
479 *Virol J*. 2011;8(1):449.
- 480 [65] Williams DT, Daniels PW, Lunt RA, Wang LF, Newberry KM, Mackenzie JS. Experimental  
481 infections of pigs with Japanese encephalitis virus and closely related Australian flaviviruses.  
482 *Am J Trop Med Hyg*. 2001;65(4):379-87.